ELASTIC LOOP MOBILITY SYSTEM—
A NEW CONCEPT FOR PLANETARY EXPLORATION

N. C. Costes* and W. Trautwein†

INTRODUCTION

SURFACE mobility by advanced roving vehicles will be the key to augmenting the scientific return from future lunar and planetary missions over large areas. Wheeled rovers provided sufficient mobility for the early phase of lunar exploration as demonstrated by the successful Lunokhod 1, Apollo 15 and 16 missions [1, 2].

For the more ambitious rover missions, associated with manned or automated exploration over extended periods of time, maximum mobility and reliability is desirable to find access to areas of highest scientific interest such as lunar or Martian craters and canyons. To meet this challenge, a novel mobility concept, designated as the Elastic Loop Mobility System (ELMS), has been developed by the Lockheed Missiles & Space Company (LMSC) under the sponsorship and general technical direction of the Marshall Space Flight Center (MSFC), which combines major advantages derived from both wheeled and tracked vehicles.

In the following three sections of this paper the major ELMS design characteristics are presented. Results of recent mobility performance tests are given in the fifth section followed by a discussion of possible vehicle designs, including stowage and deployment concepts.

2. MAJOR DESIGN FEATURES OF ELASTIC LOOP

Almost 40 years ago an English inventor, J. G. A. Kitchen [3] proposed continuous tracks, made of a highly elastic material, which would stiffen along the straight sections due to a preformed transverse curvature, as shown in Fig. 1. This continuous and endless track eliminates several sources for internal friction and mechanical complexity because no bogie wheels or track links are required. The tight fit between rollers and track poses a high risk of jamming and internal losses caused by the continuous crushing of foreign particles trapped between track and rollers. Attempts by Bendix to apply a continuous track concept to a small unmanned Surveyor Lunar Roving Vehicle (SLRV) were not successful.

In the ELMS concept the elastic loop performs a dual function, namely:
(1) It distributes the load over a large footprint without bogie wheels,
(2) It provides spring suspension, using the two 180-deg bends of each loop as suspension springs (Fig. 2).

The contact between the inner drums and the elastic loop is reduced to small sections in the "clean" upper third portion of the loop which remains relatively free of soil

*Staff Scientist, NASA-George C. Marshall Space Flight Center, Huntsville, Alabama.
†Staff Scientist, Lockheed Missiles & Space Company, Inc., Huntsville, Alabama.
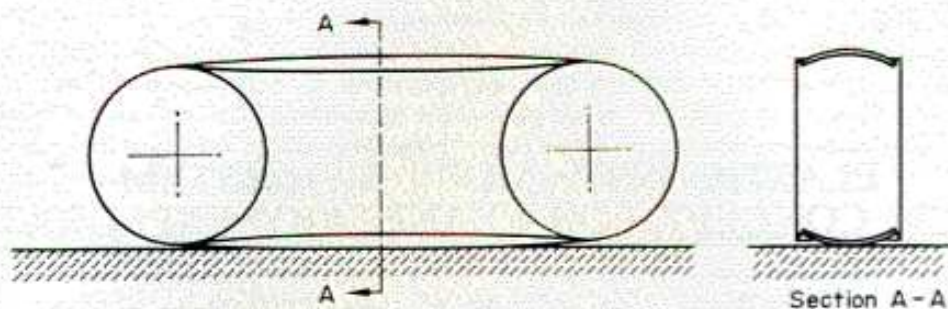
FIG. 1. Continuous track proposed by Kitchen [3] is supported by two inner rollers.
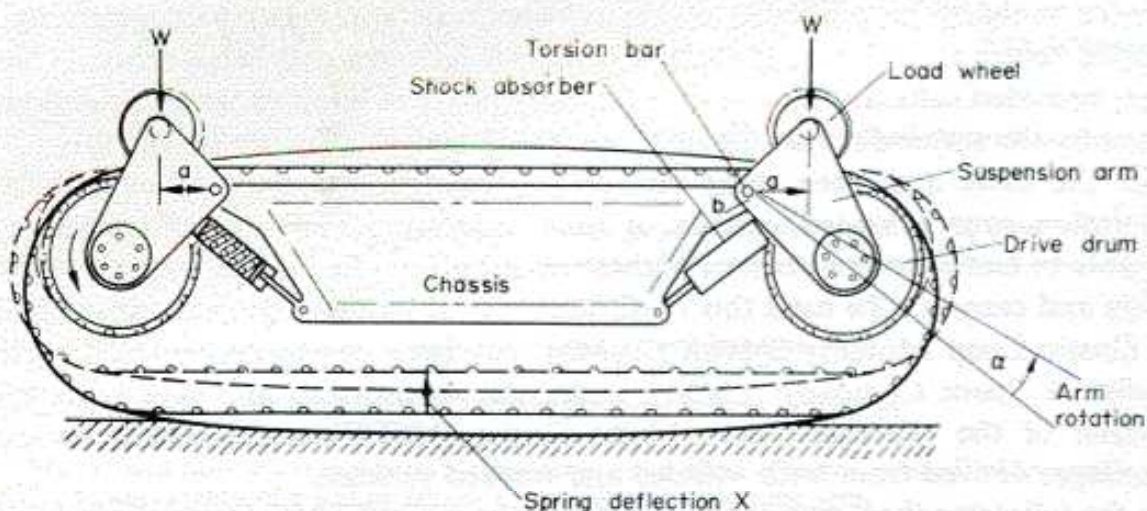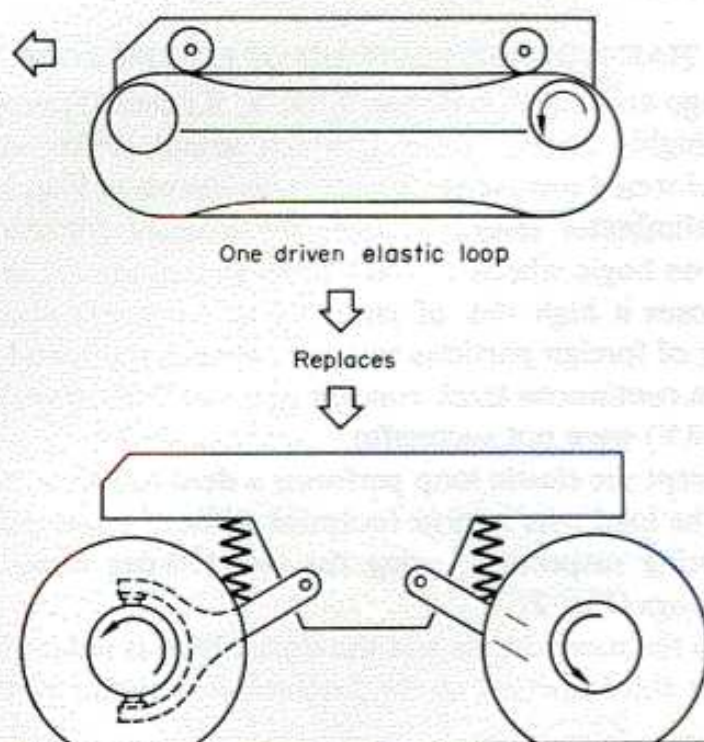

FIG. 2. ELMS concept. Vehicle weight transmitted by load wheel. Moment W*a* keeps drive drum(s) in contact with loop. Spring deflection *X* causes arm rotation α.

One driven elastic loop

Replaces

Two driven conventional wheels, spring suspension and steering mechanism

FIG. 3. Elastic loop concept simplifies vehicle design.

particles or other foreign matter. The suspension arms follow the loop as it extends under increased load. This suspension concept can absorb both vertical and horizontal impacts. Also, through this scheme, the risk of jamming caused by the entrapment of soil particles is virtually eliminated and the overall vehicle design can be substantially simplified, as illustrated in Fig. 3. The reduced number of driven wheels and the elimination of separate wheel suspension and steering systems result in major savings in mechanical parts.

3. ELASTIC LOOP STRESS-DEFORMATION CHARACTERISTICS

Loop sizing and prediction of maximum stress conditions developed in the ELMS have been based on a simplified theory which takes into account the fabrication sequence employed in the manufacturing of the elastic loops [4].

The current state of the art includes methods for producing continuous elastic loops that are made of wound fiber glass. However, thus far, all prototype test loops have been manufactured only of titanium alloy. The fabrication sequence of titanium loops includes: (1) welding of flat strips (under 45 deg); (2) bulge-forming; (3) age-hardening; and (4) roll-forming [4].

The predominant deformations of the loop are inextensional bending distortions. Accordingly, denoting the unloaded and loaded conditions by superscripts (0) and (1), respectively, and assuming the empirical relationship

$$K_q^{(1)} - K_q^{(0)} \simeq K_b^{(1)} - K_b^{(0)}, \tag{1}$$

between the transverse curvature K_q and longitudinal curvature K_b (Fig. 4) to hold, the following load-deflection characteristics are obtained

$$F^{(1)} = \pi \, b \, B(K_b^{(1)})^2 \left[1 - \frac{K_b^{(0)} + (K_b^{(1)} - K_b^{(0)})}{K_b^{(1)}} \right], \tag{2}$$

in which F = applied load (N); b = loop width (cm)

and

$$B = \frac{Et^3}{12(1 - v^2)} \quad \text{is the loop's bending rigidity,}$$

where E = Young's modulus (N/cm²); v = Poisson's ratio; t = loop thickness (cm).
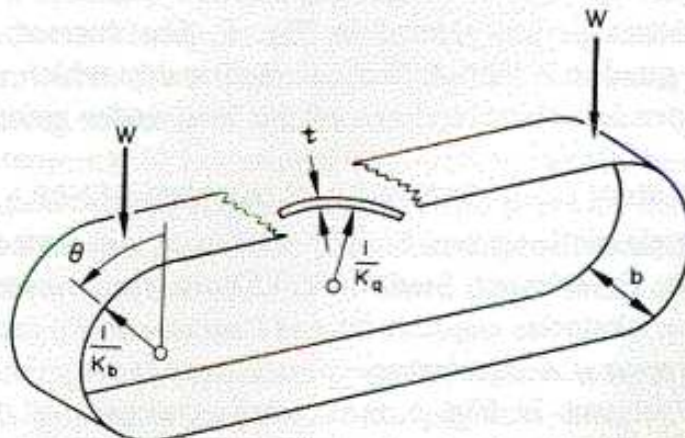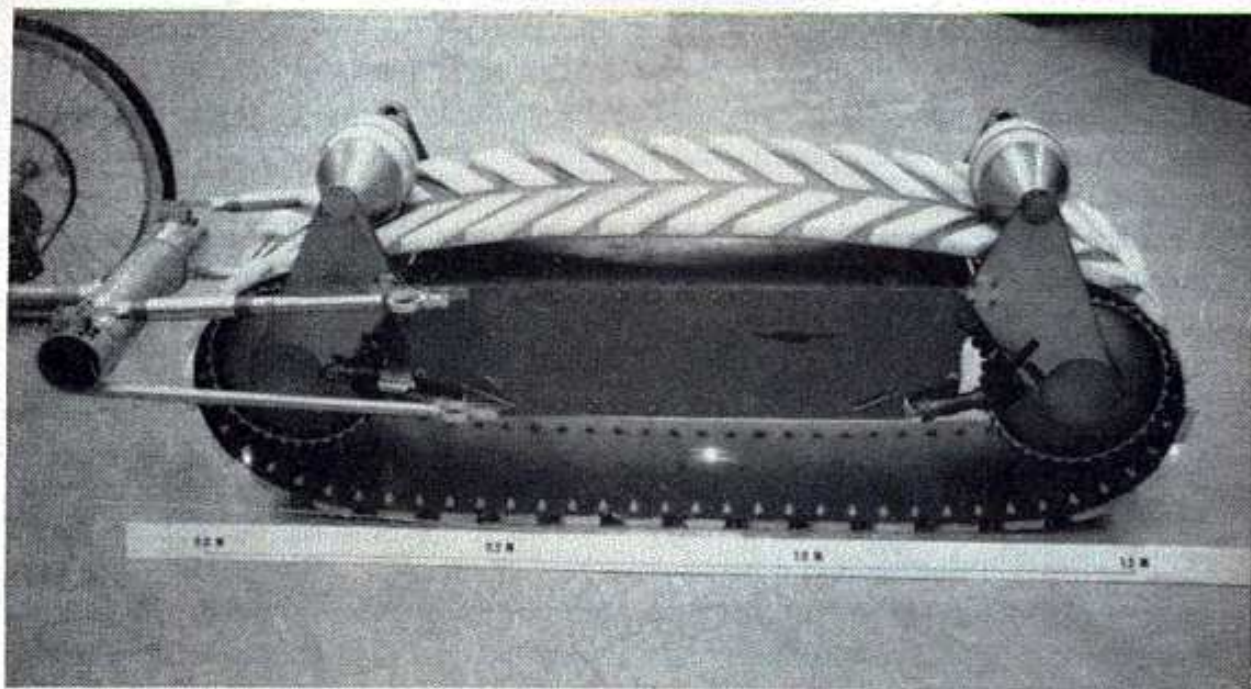

FIG. 4. Configuration of loaded elastic loop.

FIG. 5. Second-generation ELMS test unit features: (1) uniform ground pressure distribution (indicated by straight lower edge); (2) up to 150 lb (670 N) load capability; (3) Brushless d.c. motors; (4) onboard battery power, telemetry; and (5) remote control and instrumentation for performance evaluation.

Similarly, the maximum stress, σ_{max}, can be predicted from

$$\sigma_{max} = \frac{6B}{t^2}\left[K_b^{(1)} - K_b^{(c)} - K_q^{(c)} \right], \tag{3}$$

where the superscript (c) denotes "loop in circular form". Substituting in equations (1), (2) and (3) the design data (see Appendix A) for a second-generation elastic loop test unit (Fig. 5), which was built recently for MSFC's Geotechnical Research Laboratory, the following relations result:

$$F^{(1)} = 4.69 \times 10^5\, K_b^{(1)} \left[0.7\, K_b^{(1)} - 0.0166 \right]\ (N) \tag{4}$$

and

$$\sigma_{max} = 8.7 \times 10^5 \left[K_b^{(1)} - 0.0173 \right]\ (N/cm^2). \tag{5}$$

Both of these relationships are plotted in Fig. 6. The current elastic loop design features a desirable quadratic load-deflection relationship which results in increasing stiffening of the suspension characteristics of the loop under increasing load.

4. MAJOR DESIGN IMPROVEMENTS OF SECOND-GENERATION ELMS

A first-generation elastic loop was built in 1970 and was tested at the U.S. Army Engineer Waterways Experiment Station (WES) for the purpose of assessing its soft-soil performance, obstacles negotiation and slope-climbing capabilities [5]. On the basis of those tests, several design improvements were incorporated into the second-generation test unit, shown in Fig. 5. The most important of these improvements are outlined below.
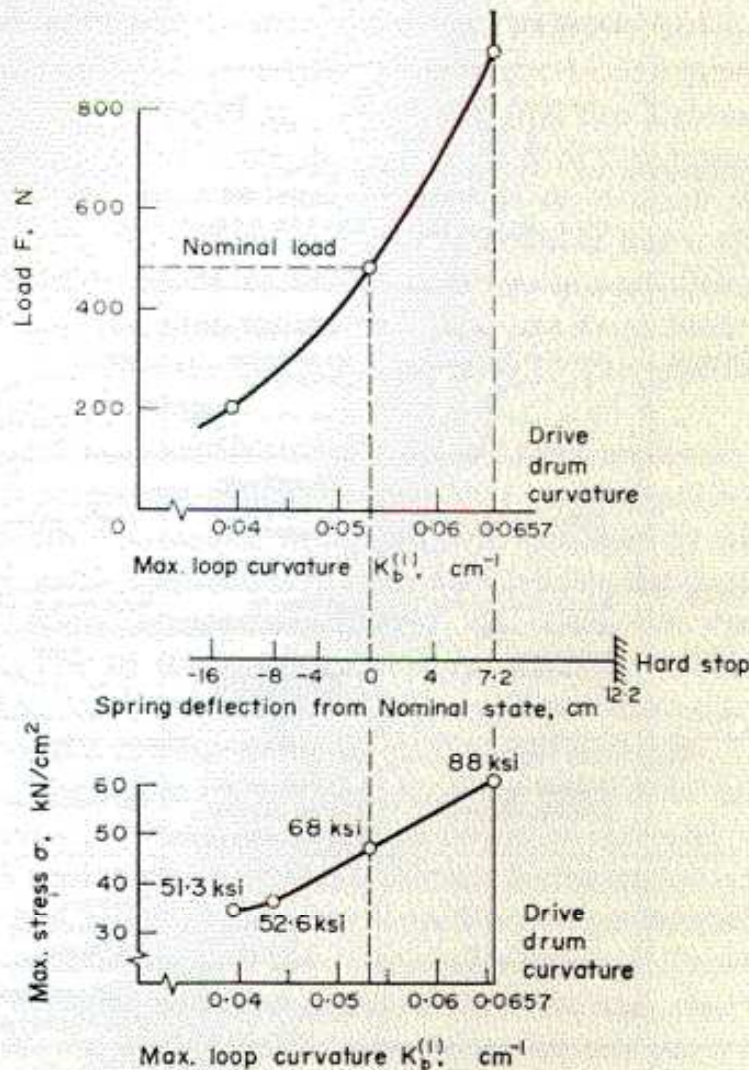
FIG. 6. Predicted spring-deflection and stress characteristics of second-generation loop shown in Fig. 5.
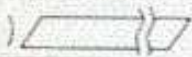
Loop manufacturing process

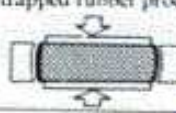The sequence of operations for the manufacture of first and second generation loops is summarized in Table 1.

A standard annealed titanium alloy was used for the first-generation loop (Table 1). After welding the sheet into a ring form and trimming to width, the forming operation was performed in a specially built single-stand roll-forming machine. The resulting loop shape is characterized by upper and lower straight longitudinal sections which are stiffened by the transverse curvature. The two flattened 180-deg end sections can be used to provide spring suspension for the vehicle.

The major shortcomings of first-generation loops were: (1) the edges were cambered along the straight sections; (2) the resulting ground pressure distribution varied substantially along the footprint, with high pressure regions fore and aft, and low or zero pressure in the mid-section near the edges. Thus, major areas of the loop's footprint were not contributing to the tractive effort.

The full-size second-generation elastic loop is made of a new titanium alloy which increased its load-carrying capability. Best physical material characteristics are achieved by age-hardening of the welded loop under controlled temperature conditions.

TABLE 1. SUMMARY OF PAST AND PRESENT LOOP MANUFACTURING PROCESSES.

	First generation Full size	Second generation 1:6 scale	Full size (Fig 5)
Material	Ti-6 Al-4V annealed	Loops No.1 and No. 2 and 1:6 scale: Ti-11·5 Mo-6·5 Zr-4·6 Sn (Beta III) Loop No.3: Ti-2 Al-11·5 V· 2 Sn-11 Zr (Transage 129)	
Manufacturing Step 1	TIG weld sheet into ring form	Brake-bend sheet for transverse curvature	TIG-weld sheet into ring form
Step 2	Trim to width (14in.)	EB-weld strip into ring form	Trim to width (16in.)
Step 3	Roll-form for transverse curvature using Roll-former	Bulge-form by trapped rubber process	Bulge-form by hydraulic bladder process
Step 4	Drill and assemble drive lugs and grousers	Drill and assemble drive lugs and grousers	Age harden and descale
Step 5			Roll-form for transverse curvature using Roll-former
Step 6			Drill and assemble drive lugs and grousers

The new loop form results in more uniform ground pressure distribution and, therefore, improved mobility in soft soil. Second-generation loops require a bulge-forming operation in addition to the uniaxial bending, as obtained from the roll-forming or from brake-bending, the latter process being mainly applicable to small-scale models (Table 1).

Bulge-forming of full-size loops was achieved by means of a special tool which was developed in co-operation with MSFC's Process Engineering Laboratory. Similar to the trapped-rubber forming process, which is used successfully in scale-model loop fabrication (Table 1), the welded loop was pressed radially into an outer die whose inner wall was contoured to the desired curvature.

The radial pressure was applied by a water-filled rubber bladder connected with a 1000 psi pump. During bulge-forming, the tool assembly was mounted onto the MSFC's Lake Erie press, and was subjected to a press load of 400-600 tons which kept the pressurized bladder chamber closed.

The experience gained in this loop manufacturing effort has led to an improved manufacturing technique, combining the bulge-forming with the age-hardening operations, that promises more uniform loops at reduced cost.

Drive system modification for higher efficiency and torque requirements

The first-generation ELMS drive system was torque-limited in a number of testing modes. The second-generation ELMS is equipped with two high-performance brushless d.c.-drive motors which were developed by MSFC's Astrionics Laboratory. These motors were incorporated into the internal drive drum design forming an integral part of the two drive drums and their suspension. The total output torque of these motors is 216 N-m (160 ft-lb), exceeding the torque requirements of the ELMS test unit. The maximum motor torque has, therefore, been limited to 81 N-m (60 ft-lb). This value represents the maximum expected torque required during obstacle negotiation and slope climbing.

The two drive motors can satisfy stringent torque-speed requirements not achievable with minimum size permanent-magnet or series motors. High efficiency static controllers using pulse-width modulation were built and furnished by MSFC's Astrionics Laboratory. Pulse-width modulation is used to minimize the problem of heat dissipation and to permit regenerative braking and continuous operation with full torque, if desired. The all solid-state controllers also affect winding shifts between series and parallel motor operation. This results in a 50 per cent reduction of maximum controller current and a corresponding size and weight decrease.

The efficiency of the power transmission from the inner drive drums to the elastic loop was significantly improved by mounting arrays of planetary rollers around the drive drums which tend to eliminate sliding friction during engagement and disengagement of the drive lugs mounted along the loop. Frictionless flexural pivots have been used to minimize internal energy losses of the roller bearings. These pivots can rotate $\pm$ 12 deg during engaging and disengaging of the drive lugs, thus providing rolling contact that exceeds the predicted deflections by a wide margin.

Improved traction capabilities through large grousers

The design and manufacturing process applied in the second-generation elastic loop results in almost straight lower edge loop sections, as shown in Fig. 5. This permits the installation of large grousers that provide near uniform ground pressure across the complete width of the loop.

The material used for the grousers was polyurethane foam. This material exhibits soft spring characteristics under the expected low ground contact pressures which are lower than 0·7 N/cm^2 (1 psi). To ensure safe and simple mounting and to enhance the structural integrity of the grousers, a thin reinforcing titanium-alloy plate was moulded into each grouser. These plates were also used to mount the grousers on to the elastic loop, necessitating a minimum number of drive lugs and drilled-in holes.

Optimization of ELMS damping characteristics through adjustable shock absorbers

Two lightweight adjustable shock absorbers have been installed between the ELMS chassis and the drive drum support arms for the purpose of damping the motion of the ELMS unit in excessive pitching or vertical oscillations absorbing horizontal impact loads. The front shock absorber is visible in Fig. 5. One-way damping action is required to assure continuous contact and drive torque transmission between loop and drive drums during outward deflections of the drums.

Energy dissipated in the shock absorbers can be monitored by measuring the piston

force F and the piston travel s, using an on-board strain gaged clevis for each damper and potentiometers which have been installed inside the ELMS chassis.

5. PERFORMANCE EVALUATION OF SECOND-GENERATION SINGLE ELMS UNITS

The second-generation ELMS was completed in June 1972 and is presently undergoing extensive performance evaluation at WES. Detailed analysis of the data from this test program is beyond the scope of this paper and will be included in another forthcoming publication. However, following are highlights of some preliminary results available to date.

During the first phase of this program, the ELMS was mounted in a single-unit dynamometer system to test its soft-soil performance on a level surface. Instrumentation provided for continuous recording of load, pull, torque, speed, slip, pitch moments under restrained pitch angles, and force displacement occurring at its shock absorbers. In addition, sinkage and pitch angles were recorded, the latter when the unit was allowed to pitch freely during a test. The unit was tested under applied loads of 565 N (126 lb) and 690 N (154 lb). The speeds of the ELMS and the dynamometer carriage were varied to develop slips ranging between −5 per cent and 80 per cent; the ELMS speeds were about 0·5 and 1·9 m/sec.

The system was tested on a crushed-basalt lunar soil simulant (LSS) at two consistencies: one in which the soil was placed air-dry and loosely, thereby exhibiting relatively high compressibility and low strength characteristics, and one in which the soil was placed moist and was compacted to attain a relatively high strength and penetration resistance. These two soil consistencies were attained under carefully controlled conditions so as to allow a direct comparison with the soft-soil performance of the wire-mesh wheels of the U.S. Lunar Roving Vehicle (LRV), which recently had been evaluated on the same LSS [6].

Typical results of a programmed slip test on level ground (test No. 005-6) are plotted in Figs. 7 and 8 and can be compared with the first-generation ELMS and with the LRV-wheel performance [6] for the same soil condition (LSS$_2$). This comparison shows that the performance of the current ELMS is decisively superior to that of the LRV wire-mesh wheel.

The dramatic improvement in soft-soil traction from the first to the second-generation ELMS must be attributed to the new loop-forming technique, which employs bulge-forming prior to age-hardening and roll-forming of the loop, thus eliminating the longitudinal bow across the lower edge sections of earlier loops.

During the second phase of the program, the capability of the ELMS to climb soft-soil slopes was assessed. For these tests a two-wheel trailer was mounted to the rear of the ELMS (Fig. 9) to give it the necessary stability; the vehicle was remotely controlled. Instrumentation which was provided partly by a telemetry system and partly by cables transmitted continuous recording of pull; torque; speeds; slip; pitch moments at the connection between ELMS and trailer; and energy dissipation. The soil was the same lunar soil simulant, prepared to the two strength levels that were used during the first phase of the program. Slope angles ranged from 0 to 35 deg. The ELMS was able to climb an equivalent maximum slope of 31 deg. on low-strength soil and 35 deg on high-strength soil. In both cases, the results agreed quite well with the maximum slopes predicted from level-surface tests.
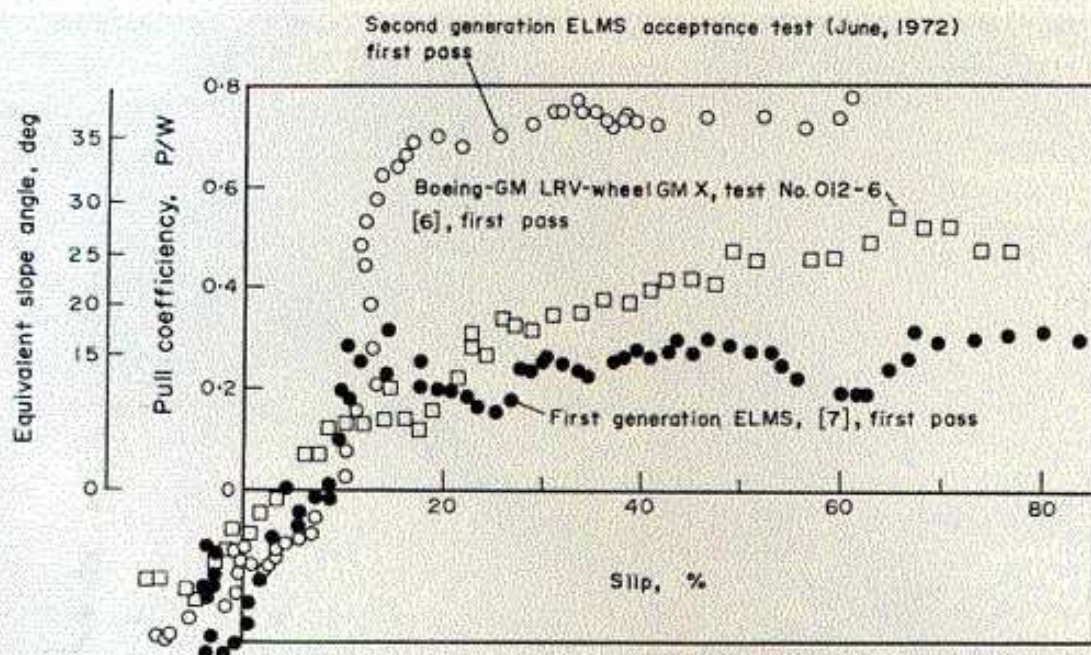
FIG. 7. Comparison of preliminary results of typical WES/acceptance test (No. 72-005-6) on level surface for second-generation ELMS with Boeing-GM LRV-wheel and first-generation ELMS in same test facility and soil condition.
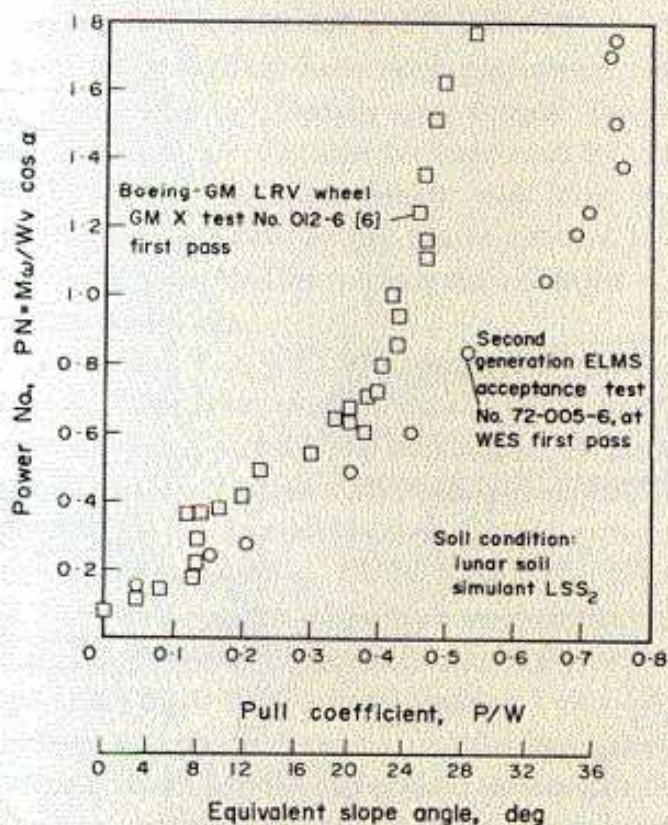

FIG. 8. Power number as a function of drawbar pull or equivalent slope for second-generation ELMS and for Boeing-GM LRV-wheel. M = wheel torque; P = drawbar pull; W = wheel load = (57 lb LRV; 127 lb ELMS II); ω = angular velocity; v = translational speed; α = slope angle.
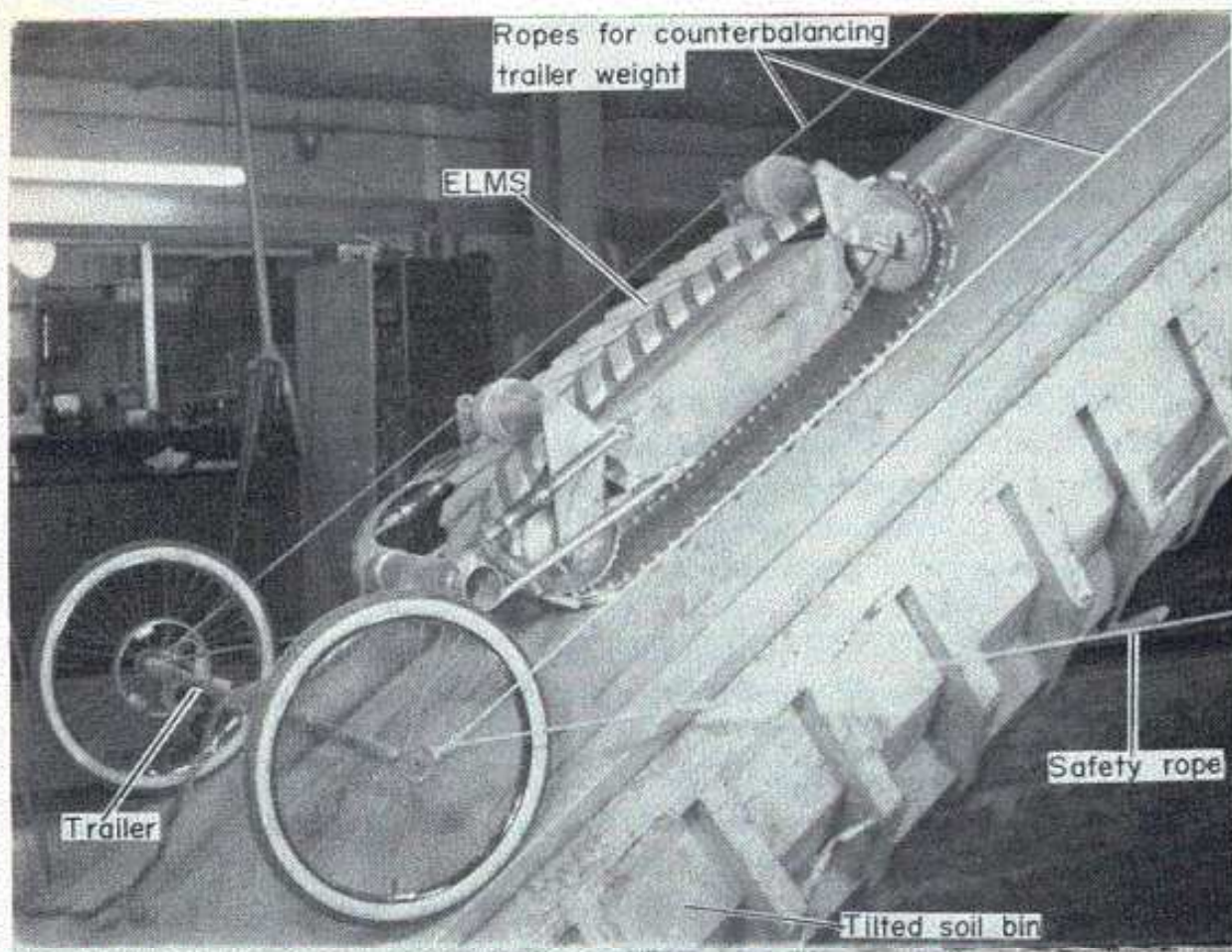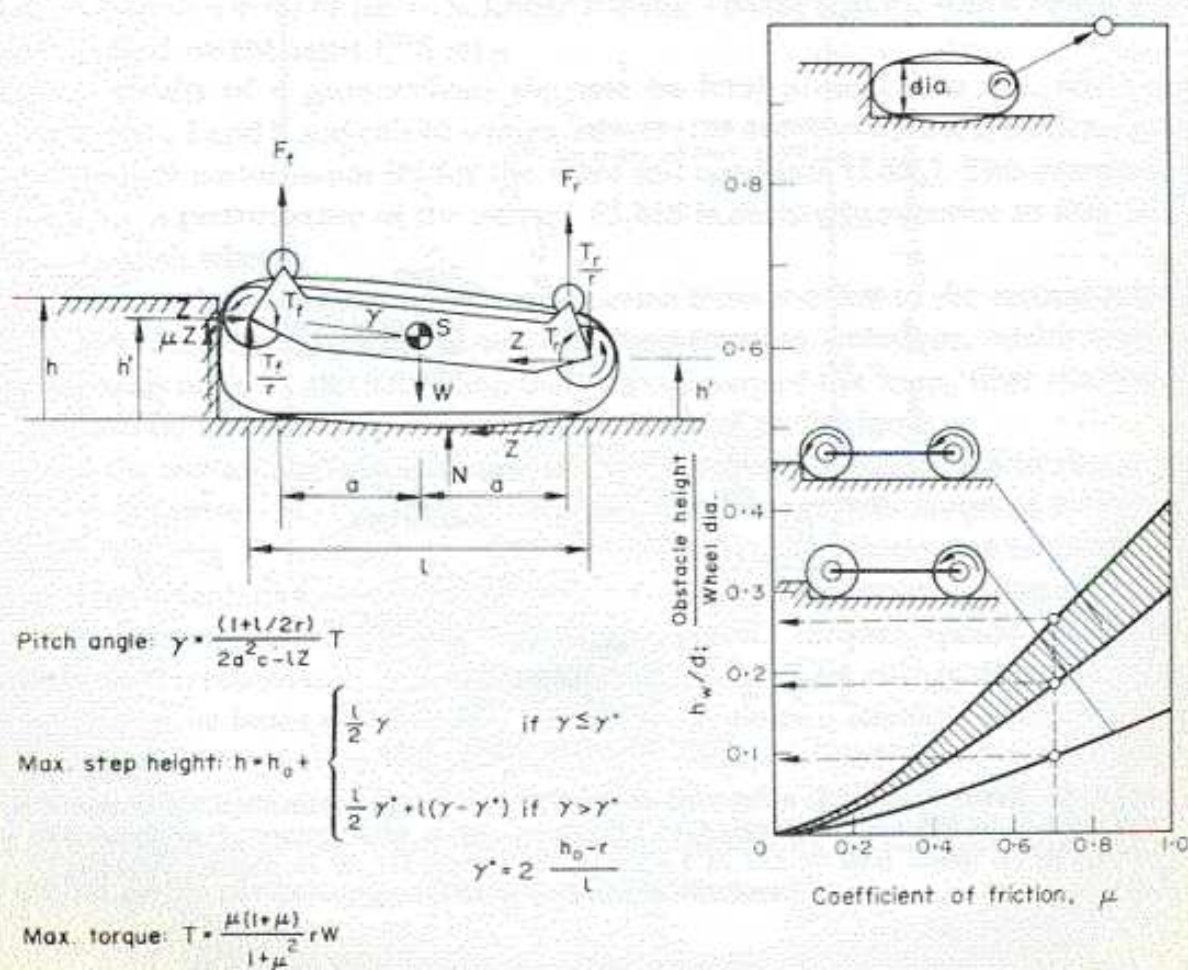
FIG. 9. ELMS-trailer configuration on 34-deg slope.

Pitch angle: $\gamma = \dfrac{(1+l/2r)}{2a^2c - lZ} T$

Max. step height: $h = h_a + \begin{cases} \dfrac{1}{2}\gamma & \text{if } \gamma \leq \gamma^* \\[2mm] \dfrac{1}{2}\gamma^* + l(\gamma - \gamma^*) & \text{if } \gamma > \gamma^* \end{cases}$

$\gamma^* = 2\,\dfrac{h_a - r}{l}$

Max. torque: $T = \dfrac{\mu(1+\mu)}{1+\mu^2}\, rW$

FIG. 10. ELMS obstacle climbing capability.

The third phase of the program consisted of tests during which the ELMS had to negotiate rigid obstacles and to cross simulated crevasses. The same ELMS-trailer configuration and recording methods were used as in the slope-climbing tests. The maximum height of negotiated step obstacles was 46 cm. This step height, which was negotiated by a single loop with passive trailer, exceeds the capability of a conventional track of the same geometry, as analyzed by Kühner [8], by almost 100 per cent. The maximum step height that can be negotiated by a conventional tracked vehicle under nominal load is less than the height of the front sprocket's center. For a tracked vehicle having the ELMS dimensions, this height would be about 23 cm above ground.

As illustrated in Fig. 10, the elastic suspension of the chassis in the loop plays a major role in this improved obstacle climbing capability. The drive torque forces the chassis to pitch nose up, deflecting the rear portion of the loop. The front wheel tends to climb up the vertical section of the loop, virtually independent of the coefficient of friction at the wall. The results of a first-order analysis of chassis pitch angle, step height and torque requirements are also given in Fig. 10. The substantial advantage of the ELMS over 4 × 2 and 4 × 4 wheeled configurations is evident in the plot where results by Rettig and Bekker [9] for wheeled vehicles are compared with the recent test result of the second-generation ELMS. Comparing wheels with an elastic loop the height of which is equal to the wheel diameter shows a 3 : 1 advantage over 4 × 2 vehicles. Preliminary tests with an articulated dual-unit 3-loop ELMS vehicle indicate that step obstacles as high as the length of the loop can be negotiated by 3 × 3 or 4 × 4 ELMS configurations.

6. ELMS ROVER CONFIGURATION

Initial feasibility and design studies have been performed concerning 2 × 2 con-figurations (Fig. 11), which are mechanically very simple. Two drive motors provide full mobility and steering. Ride quality can be improved by counteracting walking-beam suspension of the loops. The space inside each loop provides ideal stowage compartments for payload. Their low height above ground keeps the c.g. low and provides ready access to the surrounding surface for scientific equipment such as soil samplers, magnetometers and drills.

For high payload capability, 4 × 4 ELMS rovers with pitch-yaw-roll articulation between the 2 × 2 units have been evaluated (Fig. 12). An attractive concept for medium payloads consists of a 2 × 2 ELMS unit linked by pitch and yaw joints to a single loop front unit, as shown in Fig. 13. Although virtually equal to the 4 × 4 ELMS in mobility, the articulated 3 × 3 configuration can be stowed as a very compact package during launch, as shown in Fig. 14, by sliding the front unit under the rear unit's center chassis. For deployment, the front unit drives under its own power, guided in a rail, and links up with the rear unit near the yaw joint. This represents a very compact stowage and simple deployment concept. For a given stowage height H in the launch or landing vehicle, and ruling out folding schemes because of their complexity in deployment, an ELMS unit of typical proportions will provide 5·5 times more footprint area than a single wheel or 2·75 times more footprint than two wheels (Case A in Fig. 15). Similarly, if the stowage volume V is specified (Case B in Fig. 15) there is again a 5·1 times larger footprint possible for an ELMS, if compared with a wheel, and a 2·55 times larger footprint, if a single elastic loop is to replace two wheels.
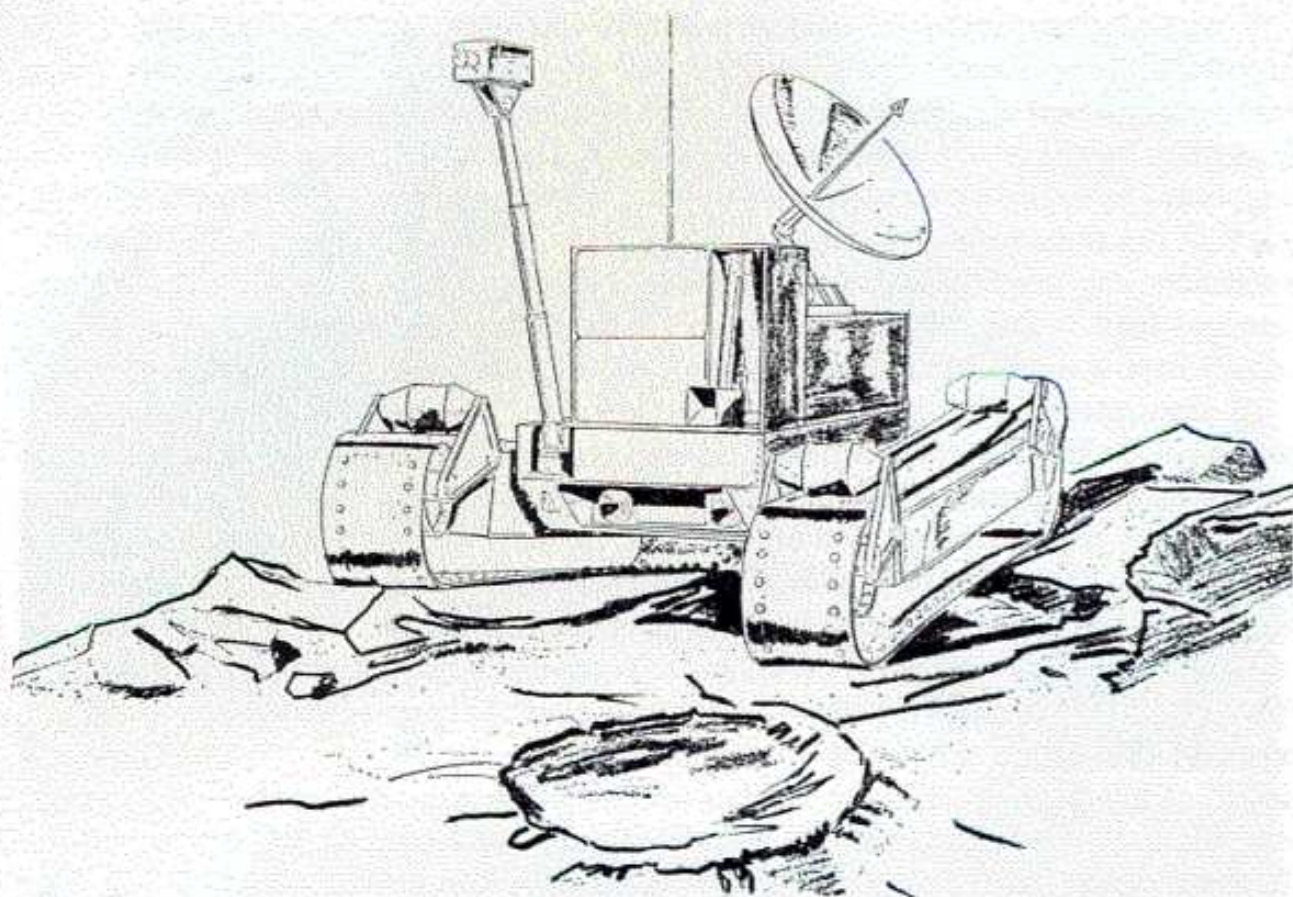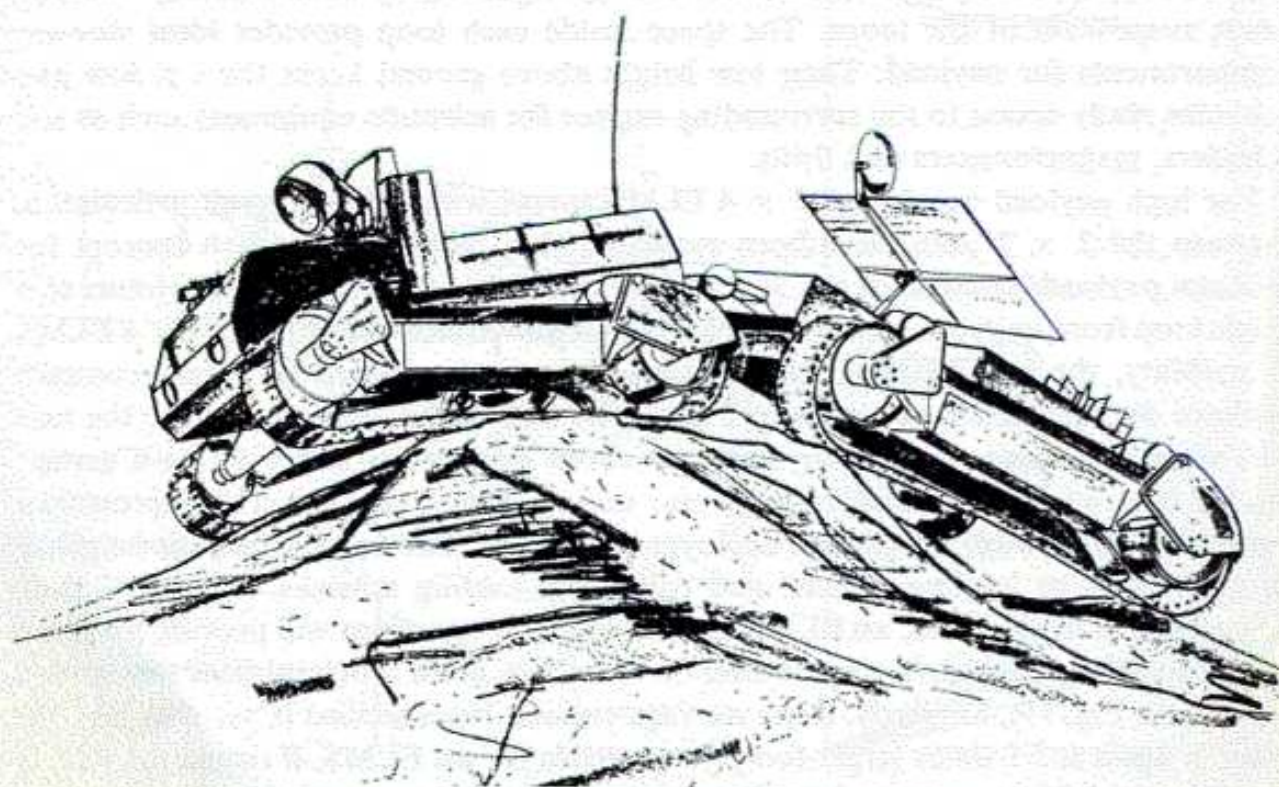
Fig. 11.   2 × 2 ELMS configuration.

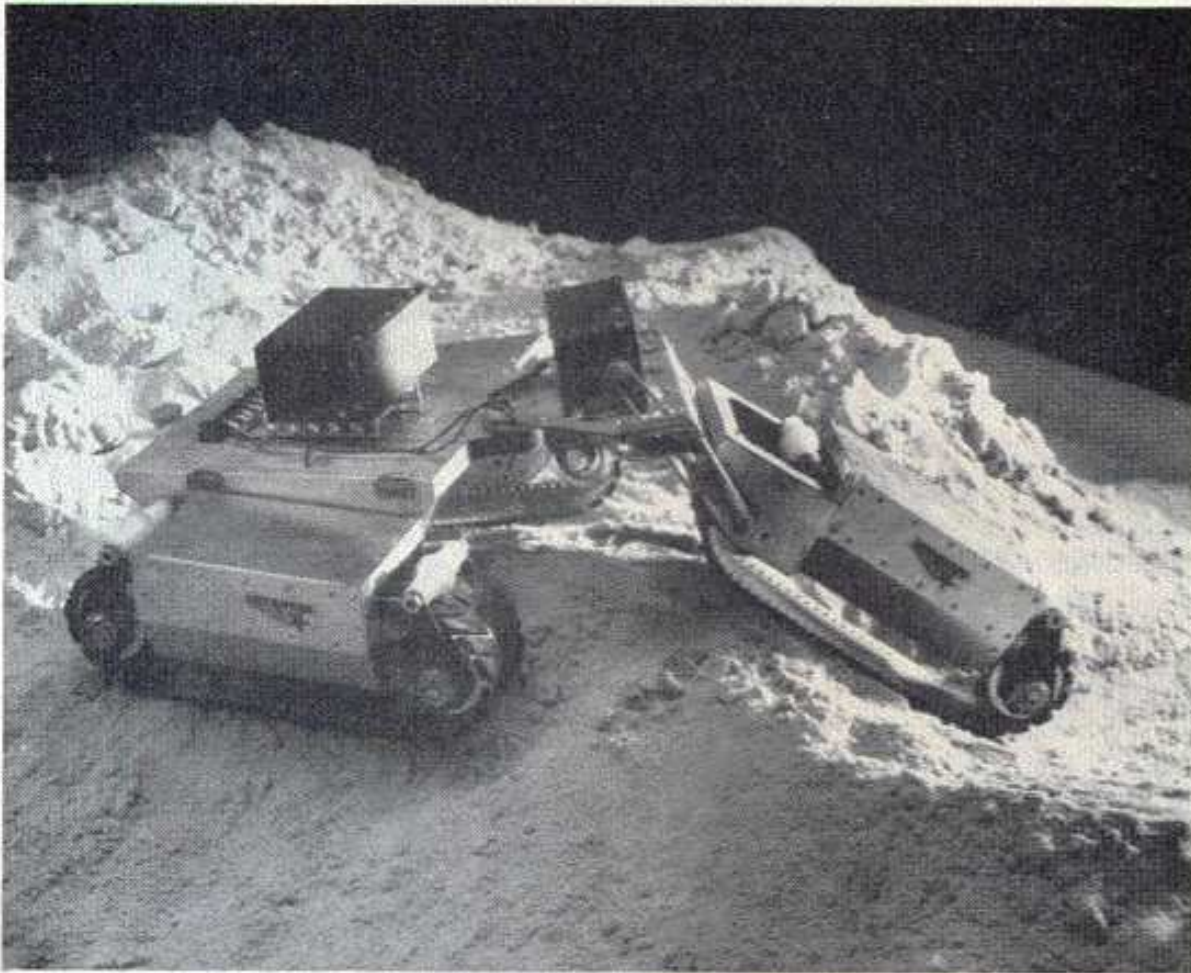Fig. 12.   4 × 4 Articulated ELMS configuration.

FIG. 13. Self-powered model of 3 × 3 ELMS Roving Vehicle with active pitch articulation and yaw steering built for MSFC's Geotechnical Research Laboratory.

FIG. 14. Simple yet compact 3 × 3 ELMS stowage concept. For deployment front unit drives forward under its own power.
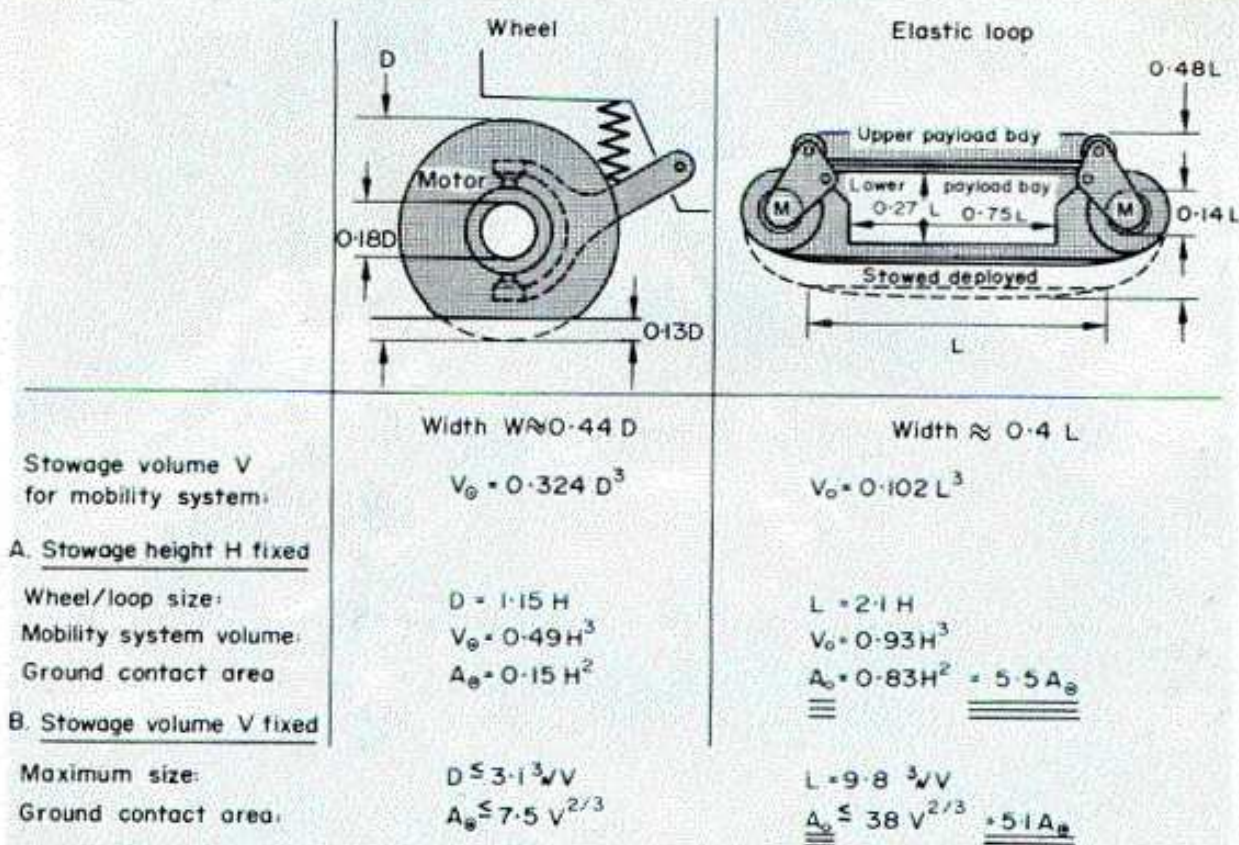
	Wheel	Elastic loop
	Width $W \approx 0.44\,D$	Width $\approx 0.4\,L$
Stowage volume V for mobility system:	$V_\ominus = 0.324\,D^3$	$V_o = 0.102\,L^3$
A. Stowage height H fixed		
Wheel/loop size:	$D = 1.15\,H$	$L = 2.1\,H$
Mobility system volume:	$V_\ominus = 0.49\,H^3$	$V_o = 0.93\,H^3$
Ground contact area	$A_\ominus = 0.15\,H^2$	$A_o = 0.83\,H^2 = 5.5\,A_\ominus$
B. Stowage volume V fixed		
Maximum size:	$D \leq 3.1\,\sqrt[3]{V}$	$L = 9.8\,\sqrt[3]{V}$
Ground contact area:	$A_\ominus \leq 7.5\,V^{2/3}$	$A_o \leq 38\,V^{2/3} = 5.1\,A_\ominus$

FIG. 15.   Comparison of mobility system size and stowage volume.

Height of c.g.: $H_o = 0.7\,G_o$

Science deployment travel: $S_o = 0.3\,G$

$H_\ominus = 1.3\,G_\ominus$

$S_\ominus = G_\ominus$
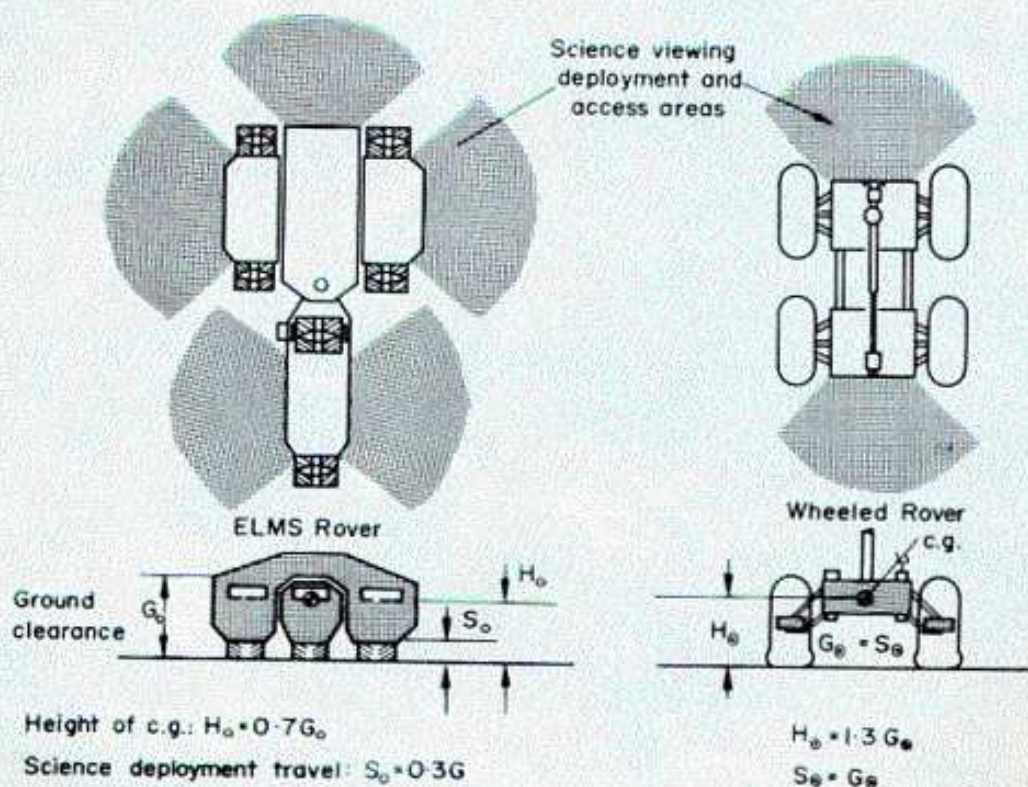
FIG. 16.   Comparison of science accessibility and static stability.

The front unit of the 3×3 ELMS can perform an important function during autonomous operation on a distant planet: In combination with a simple pitch angle sensor and a vertical reference it acts as a tactile hazard detector. If the allowable pitch angles are exceeded the vehicle stops and pulls back. In contrast, were this concept to be applied to a wheeled rover, five or six wheels would have been required.

A number of additional properties which can augment the scientific return of a future rover mission are depicted in Fig. 16. The widely distributed payload compartments provide for ideal science deployment, accessibility and viewing range by imagery. For a given ground clearance G and vehicle width, the static lateral stability is $0.7\ G$ for a typical 3×3 ELMS and $1.3\ G$ for a wheeled rover.

Soil samplers and other experiments which must make contact with the surface can be deployed from the bays inside the loops, thus reducing the travel distance S for deployment by typically 70 per cent (from $S = G$ for wheeled rovers to $S = 0.3\ G$ for ELMS rovers).

7. CONCLUSIONS

The Elastic Loop Mobility System (ELMS) combines the traction capabilities of tracks with the light weight and relatively low energy consumption of wheels. Major design rules have been derived through which roving vehicles of very simple, stable and reliable design can be built. Such vehicles would be ideally suited to extended lunar or planetary missions.

Extensive soft-soil performance and obstacle-negotiation tests of a full-scale single ELMS loop have been performed. Preliminary analysis of these tests indicates that the mobility performance of single ELMS units is by far superior to the performance of single wire-mesh wheels of the Lunar Roving Vehicle. To establish adequate confidence limits on performance and design data relating to future rover mission planning, the present tests should be supplemented by mobility tests of 2×2 and 3×3 ELMS prototype test vehicles.

APPENDIX A

The major design data of the second generation ELMS are as follows:

Loop width: $b = 38 \cdot 8$ cm
Loop thickness: $t = 1 \cdot 6$ mm
Loop circumference: $L = 3 \cdot 68$ m
Overall loop length
under nominal load: $1 \cdot 6$ m
Weight of assembled
loop (incl. grousers): $= 148$ N (33 lb)
Material: Ti—11·5 Mo—6·5 Zr—4·6 Sn (Beta III)

Young modulus, $E = 10 \cdot 3 \times 10^6$ N/cm² (15×10^6 psi)

Poisson's ratio, $\nu = 0 \cdot 3$

REFERENCES

[1] N. C. COSTES, J. E. FARMER and E. B. GEORGE, Mobility performance of the lunar roving vehicle. Terrestrial studies—Apollo 15 results. *Proc. Int. Conf. of the International Society for Terrain-Vehicle Systems*, Vol. I, pp. 34–35 and Vol. III, Stockholm (1972).
[2] J. K. MITCHELL, L. G. BROMWELL, W. D. CARRIER, N. C. COSTES, W. N. HOUSTON, and R. F. SCOTT, Soil mechanics experiment Apollo 15 preliminary science report, Chapter 7, *NASA SP* 289 (1972).
[3] J. G. A. KITCHEN, Endless traveler band, track and the like *U.S. Pat.* 2,055,932, (1933).
[4] W. TRAUTWEIN, Design fabrication and delivery of an improved single elastic loop mobility system. *Report* No. LMSC-HREC D225600-II (1972).
[5] K. J. MELZER and W. TRAUTWEIN, Performance characteristics of a first-generation elastic loop mobility system. *Proc. 4th Int. Conf. of the International Society for Terrain–Vehicle Systems*, Vol. I, pp. 83–98, Stockholm (1972).
[6] A. J. GREEN and K. -J. MELZER, Performance of the Boeing LRV wheels in a lunar soil simulant; effect of wheel design and soil. *Report* No. TR M-71-10, U.S. Army Engineer Waterways Experiment Station, Corps of Engineers, Vicksburg, Miss. (1971).
[7] K.-J. MELZER and A. J. GREEN, Performance evaluation of a first-generation elastic loop mobility system. *Report* No. TR-M-71-1, U.S. Army Engineer Waterways Experiment Station, Vicksburg, Miss. (1971).
[8] K. KÜHNER, Das Kraftfahrzeug im Gelände. *Z. Ver. dt. Ing.* **79**, 1019-1027 (1935).
[9] M. G. BEKKER, *Theory of Land Locomotion*, p. 384. University of Michigan Press, Ann Arbor (1956).